Synthesis of aluminophosphate-type molecular sieve MgAPO-36 (ATS) by dry-gel conversion (DGC) method and its application of shape-selective catalysis

Shyamal Kumar Saha, Hiroyoshi Maekawa, Yoshihiro Kubota, and Yoshihiro Sugi[*]

Department of Materials Science and Technology, Faculty of Engineering, Gifu University, Gifu 501-1193, Japan

Tel. & Fax: +81-58-293-2597, E-mail address: sugi@apchem.gifu-u.ac.jp (Y. Sugi)

MgAPO-36 (ATS topology), which is one of metallo-aluminophosphate molecular sieves, was successfully synthesized by means of dry-gel conversion (DGC) method. Characterization was performed by XRD, NH_3-TPD, TG, SEM, N_2 adsorption, and ICP analyses. MgAPO-36 has the Brønsted acidic character by the substitution of aluminum with magnesium. The selectivity for 4,4'-DIPB was about 30-35 % among DIPB isomers in the isopropylation of biphenyl: this value is quite low in comparison with MOR. Because the selectivity is higher than the composition in equilibrium, the catalysis is controlled by the pores of MgAPO-36. The differences of the selectivity are not due to their pore entrance but to differences in their pore structure. The cavity in ATS channel can not sufficiently control the transition state to form 4,4'-DIPB.
Keywords: MgAPO-36; dry-gel conversion (DGC); isopropylation; biphenyl; 4,4'-DIPB; selectivity

1. INTRODUCTION

Metal-substituted aluminophosphates have been the subject of a variety of studies since their synthesis was first reported by Flanigen et al.[1] The replacement of Al^{3+} by divalent or P^{5+} with tetravalent cations can lead to Brønsted acid sites, which makes these materials useful in acid-catalyzed reactions. At the same time, molecular sieves with pores comprised of 12 T-atoms (so-called 12-ring pores as well as "large-pores") are expected to be useful because they should have ability to perform catalysis and/or adsorption on organic molecules having large size corresponding to the pore diameter. MgAPO-36 (ATS topology)[2] is a magnesio-aluminophosphate having 12-ring channels along [001] with 6.5 x 7.4 Å of pore diameter and also annular side pockets.[3] Molecular sieves having ATS topology are interesting subjects to study in connection with zeolites with straight channel such as MOR, AFI, SSZ-31.[2] It is also interested in the comparison with SSZ-55, a silicate version of ATS.[4] MgAPO-36 has the structure, of which aluminum sites are partly substituted by magnesium. MgAPO-5 (AFI topology)[2] was also crystallized as impurity in the synthesis of MgAPO-36 by hydrothermal synthesis (HTS) method.[5]

We tried to utilize dry-gel conversion (DGC) method to overcome the problem.[6-8] This method is a kind of dry-synthesis where the utilization of bulk water is avoided. It can be more specifically classified into two different but interrelated methods; vapor-phase transport (VPT, as used by Kim et al.[6]) and steam-assisted conversion (SAC, as used by Matsukata et al.[8]) methods. Various aluminosilicate,[8,9] boron-[10] and titanium-substituted[11,12] silicate molecular sieves have been synthesized by DGC technique. Unlike the HTS method, synthesis by DGC allows nearly complete conversion of gel to high crystalline molecular sieve with high yield,

and involves minimization of waste disposal and reduction in reactor volume.[6] Uniform crystals with smaller particle size are also obtained by this technique.[7,11] Moreover, there are some examples in which dry conditions are essential or desired to give particular phases and properties.[7-9,11-13]

We report here the synthesis of pure MgAPO-36 by DGC technique, and discuss effects of synthetic conditions on the phase selection during the synthesis. The isopropylation of biphenyl over MgAPO-36 are also described to know relationships between their pore structure and shape-selective catalysis.

2. EXPERIMENTAL

2.1. Synthesis of MgAPO-36 by DGC method

Although both VPT and SAC methods work quite similarly in the synthesis of MgAPO-36, we only describe VPT method in this paper. A typical procedure with an initial gel composition of $0.92Al_2O_3$-$0.17MgO$-$1.0P_2O_5$-$1.8Pr_3N$-$45H_2O$ is as follows: an aqueous solution of $Mg(OCOCH_3)_2$ (1.7 mmol) was added to an aqueous suspension of aluminum isopropoxide (9.2 mmol). To this mixture, 40 % phosphoric acid (10 mmol) was added, and stirring was continued until the gel became homogeneous. The gel was then dried at 80°C in an oil bath with continuous stirring. When the gel became thick and viscous, it was homogenized manually using a Teflon rod and this was continued until it dried. The dry-gel obtained was ground into a fine powder and poured into a small Teflon cup (20 x 20 mm I.D.), which was placed in a Teflon-lined autoclave (23 ml) with the support of a Teflon holder. Pr_3N (18 mmol) as structure-directing agent (SDA) and small amount (ca. 0.3 g per 1.0 g of dry gel) of water as the source of steam were taken at the bottom of the autoclave in such a manner that these vapor sources never

2188

Synthesis of Aluminophosphate-type Molecular Sieve MgAPO-36 (ATS) by
Dry-Gel Conversion (DGC) Method and Its Application of Shape-Selective Catalysis

came into the direct contact with the dry-gel. After the crystallization, the product was washed by centrifuging and dried to give 2.65 g of as-synthesized white powder. The as-synthesized sample was carefully calcined in an air stream (50 cm^3 min^{-1}) as follows: the temperature was raised from 25 to 200°C over a period of 1.5 h, and maintained at 200°C for 2 h. Then the temperature was raised to 550°C over a period of 3 h and kept at 550°C for another 6 h, and finally cooled in ambient conditions.

2.2. Characterization

Phase purity and crystallinity of the as-synthesized samples were determined by powder X-ray diffraction (XRD) (XRD-6000, Shimadzu Corporation) with Cu Kα radiation (λ=1.5418 Å). Crystal size and morphology of the samples were determined by scanning electron microscopy (SEM) using a TOPCON ABT-60 microscope. Elemental analyses were performed by inductively coupled plasma atomic emission spectroscopy (ICP) by JICP-PS-1000 UV, Leeman Labs Inc. Nitrogen adsorption measurements were carried on a Belsorp 28SA (Bel Japan) apparatus. The acidity of the catalyst was measured by ammonia temperature programmed desorption (TPD) using BEL TPD-66 (Bel Japan).

2.3 Isopropylation of biphenyl

Isopropylation of biphenyl (BP) with propylene over MgAPO-36 was carried out in a 100-ml stainless-steel autoclave (SUS 316). In a typical reaction procedure, catalyst (0.25 g) and BP (7.7 g, 50 mmol) were placed in the autoclave and flushed with N$_2$ for several times. The autoclave was heated slowly to the desired temperature (typically 250°C) and the reaction started after the introduction of propylene. Propylene pressure kept constant at 0.8 MPa throughout the reaction (4 h). After the completion of the reaction, the autoclave was cooled; the reaction mixture was filtered and diluted to 100 ml in toluene. Approximately, 1.5 ml solution was taken from the total solution and diluted with toluene (1.5-6.0 ml). Afterwards, products were identified using GC-MS (Shimadzu QP 5000) and analyzed by gas chromatography (Shimadzu GC-14A; column: Ultra-1 (HP), 25 m x 0.3 mm).

3. RESULTS AND DISCUSSION

3.1. Synthesis

Table I shows the typical results of the synthesis of MgAPO-36 by VPT method, and Figs. 1b and 1c show the representative XRD patterns of the pure ATS phase. The XRD pattern of MgAPO-36 contaminated by MgAPO-5 (synthesized by HTS method) and the simulated pattern of MgAPO-36 are also shown for comparison in Figs. 1a and 1d, respectively. The conditions for the formation of pure ATS phases were optimized with the variation of gel compositions and heating protocol. As shown in Table 1, the phase selection was sensitive to the heating protocol. When the dry-gel was isothermally heated at 140°C or 150°C for 48 h, a mixture of ATS and AFI phases was formed (samples 1 and 2). Heating at lower temperature (105 °C) for 12-84 h caused no crystallization. Interestingly, stepwise heating at 105°C for 48 h (the first step) followed by 140°C for 24 h (the second step) gave pure ATS phase

Table I. Synthesis of MgAPO-36 by DGC method[a,b]

Sample No.	MgO/Al$_2$O$_3$[c]	Temp./°C and Time/h[g]	Product
1	0.180	140(48)	ATS + AFI
2	0.180	150(48)	ATS + AFI
3	0.180[d]	105(48)–140(24)	ATS
4	0.180	105(48)–150(24)	ATS
5	0.180	100(48)–140(24)	ATS + AFI
6	0.180	100(72)–120(72)–140(72)	ATS + AFI
7	0.100[e]	105(48)–140(24)	ATS
8	0.050	105(48)–140(24)	ATS[h]
9	0.250[f]	105(48)–140(24)	ATS[i]
10	0.326	105(48)–140(24)	AFI + impurity

[a] starting gel composition:Al$_2$O$_3$/P$_2$O$_5$=0.92, Pr$_3$N/P$_2$O$_5$= 1.8, H$_2$O/P$_2$O$_5$=40-45. [b] VPT method. [c] MgO/Al$_2$O$_3$ molar ratio in the starting gel. [d] The ratio in the product determined by ICP is 0.174. [e] 0.097 in the product. [f] 0.240 in the product. [g] Time is shown in parenthesis. [h] Crystallinity is low. [i] With trace impurity

(samples 3 and 4 in Table 1, and Fig. 1b). The slight change of temperature in the second step did not hinder the formation of pure MgAPO-36, whereas small change in the first step caused the formation of the mixture of ATS and AFI phases.

This observation prompted us to investigate the effect of the first step of the heating protocol. The heating time of the first step at 105°C (denoted t_1) was varied from 12 to 72 h, fixing the second step at 140 °C for 24 h. When t_1 was 12 and 24 h, products were ATS phase with considerable amount of AFI phase. With increasing t_1 up to 36 h, relative content of AFI decreased. Further increase in t_1 completely prevented the formation of AFI phase, leading to the crystallization of pure ATS phase when t_1=48-72 h. In case that the heating time of the second step at 140°C (denoted t_2) was varied from 12 to 72 h with fixing t_1 for 24 h, the products were always the mixture of ATS and AFI phases with no obvious tendency of the relative content. These observations
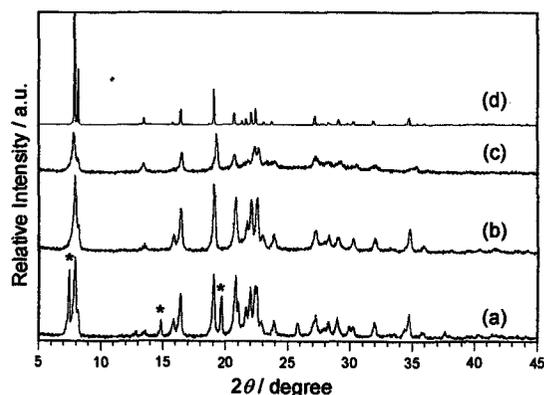

Fig. 1. Powder XRD patterns of (a) as-synthesized sample by HTS method (asterisks denote representative peaks from AFI impurity), (b) as-synthesized, pure ATS sample obtained by VPT method (sample 3 in Table 1), (c) sample (b) calcined as described in the text, and (d) simulated pattern given for comparison.
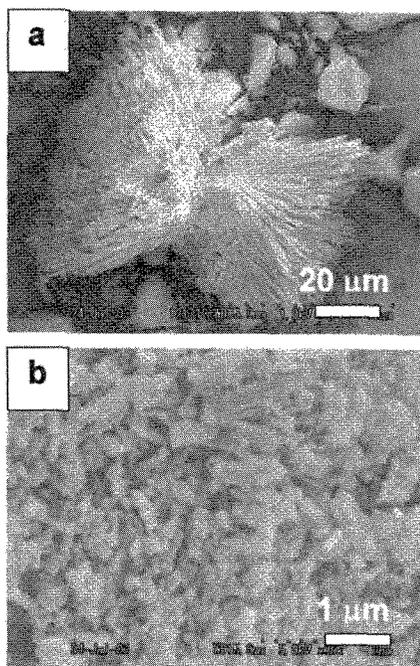
Fig. 2. SEM images of MgAPO-36 obtained by (a) HTS, and (b) VPT method.

Fig. 4. Effects of reaction temperature on conversion and selectivity for DIPB isomer. Reaction condition: BP, 50 mmol; catalyst, MgAPO-36 (MgO/Al$_2$O$_3$=0.174), 0.25 g; propylene, 0.8 MPa; period, 4 h.

suggested that there is no phase transformation from AFI to ATS (or inverse), but there should be competitive nuclei formation of the two phases, and the first step (t_1) is critical governing factor for the nucleation.

Starting MgO/Al$_2$O$_3$ ratio influenced on the phase purity of ATS (Table 1, samples 3, 7-10).[14] The ratios between 0.1 and 0.25 successfully gave pure ATS phase. When the ratio was below 0.1 or above 0.25, poorly crystalline ATS or AFI phase with other impurities were formed, respectively. Elemental analysis of the product showed that the MgO/Al$_2$O$_3$ ratio in the starting gel was retained in the as-synthesized sample, suggesting that major portion of gel phase was converted to ATS phase (Table 1, samples 3, 7, and 9).

The amount of Pr$_3$N was important and the pure ATS was crystallized only at Pr$_3$N/Al$_2$O$_3$ ratio from 0.49 to 1.96. The product was contaminated with AFI and other
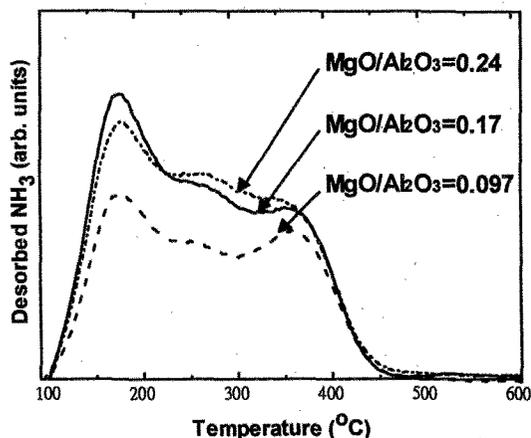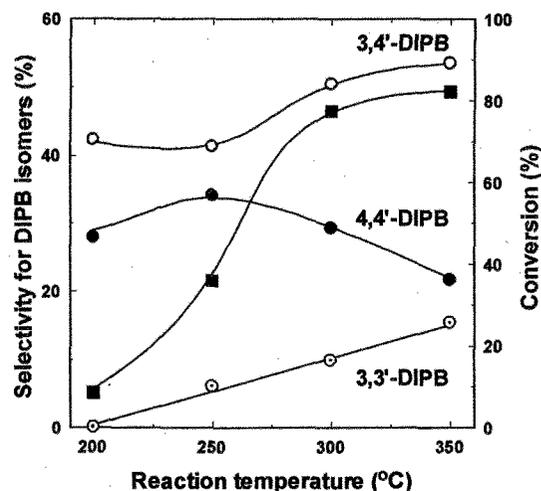

Fig. 3. Effects of NH$_3$-TPD of MgAPO-36

phase below the ratio, and further in crease of SDA enhanced the crystallization of AFI phase.

MgAPO-36 was crystallized even in the absence of external bulk water, indicating that very minute amount of water is necessary for the crystallization of ATS phase. In this case, adhered water to the dry-gel could have contributed to the crystallization. Thus, a convenient N$_2$ adsorption, methodology to synthesize pure ATS phase was established. It should be noted that the hydrothermal synthesis of pure ATS phase was still difficult even when starting from the same gel composition and under analogous conditions, giving ATS phase contaminated by AFI (Fig. 1a).

Figures 2a and 2b show SEM photographs of as-synthesized MgAPO-36 obtained by HTS and VPT methods, respectively. The sample from HTS method contains particles with different morphologies (Fig. 2a), being consistent with Fig. 1a. Needle-like crystallites as long as 40 μm are assigned to be ATS phase on the basis of particle distribution and a SEM image in cited Ref. 5. Differently, very small rod-like or spherical crystallites (0.2-0.8 μm) of ATS phase are observed in case of DGC method (Fig. 2b). Careful calcination steps as described in the experimental part were essential to obtain the reasonable porosity.

Figure 3 shows the NH$_3$-TPD of MgAPO-36 with different MgO/Al$_2$O$_3$ ratio. All of them have the peaks around 250-400°C due to strong acidic sites by substitution of aluminum with magnesium. They are expected strong enough to work for acid catalysis.

According to the N$_2$ adsorption isotherm, carefully calcined MgAPO-36 has a micropore volume of 0.16 cm^3 g^{-1} and the BET surface area of 360 m^2 g^{-1}.

3.2. The isopropylation of biphenyl

The isopropylation of BP is an acid-catalyzed reaction, which produces mixture of isopropylbiphenyl (IPBP), diisopropylbiphenyl (DIPB), and triisopropylbiphenyl (TrIPB) isomers. Detailed investigation of isopropylation of BP over MOR and other zeolites has been previously

reported from our group.[15-18] Shape-selective isopropylation occurred to yield predominantly the least bulky 4-IPBP among IPBP isomers and 4,4'-DIPB among DIPB isomers. The selectivity for 4,4'-DIPB was up to 80-90 % among DIPB isomers under mild conditions such as temperature of 250°C and propylene pressure of 0.8 MPa. 4,4'-DIPB is principally produced from 4-IPBP inside pores of MOR by restricted transition state mechanism.[15-17] We also found that some one-dimensional molecular sieves with straight channel enhanced the shape-selective isopropylation of BP.[18-20]

Figure 4 shows effects of reaction temperature on catalytic activity and selectivity for DIPB isomers in the isopropylation of BP over MgAPO-36. The conversion of BP increases with raising reaction temperature. The selectivity for 4,4'-DIPB was 25-30% in the range of 200 to 350 °C. However, the selectivity for 3,4'- and 3,3'-DIPB was 40-50% and 2-10%, respectively. The selectivity for 4,4'-DIPB decreased with the increase of 3,3'- and 3,4'-DIPB by raising reaction temperature. However, the selectivity for 4,4'-DIPB was higher than the composition in equilibrium. This means that the isopropylation of BP is controlled by the pores of MgAPO-36. However, the pores are not enough to fit for shape-selective formation of 4,4'-DIPB which occurred on MOR. It is interested that MOR and ATS has similar shape and radii of the entrance. The differences of the selectivity are not due to their pore entrance but to differences in their pore structure. ATS has one-dimensional channel with the cavity of *ca.* 1 nm,[2] however, channel of MOR is straight with side pocket. We previously proposed shape-selective formation of 4,4'-DIPB occurred inside the channel by restricted transition state mechanism over MOR. However, the reaction sites in ATS channel can not sufficiently control the transition state to form 4,4'-DIPB, and the bulkier transition state to form other bulkier isomers, such as 3,3'- and 3,4'-DIPB is also allowed inside the channel. Similar results were also found in the cases of SSZ-42 (IFR)[20] and SSZ-35 (STF).[21]

The selectivity for 4,4'-DIPB decreased and those for 3,3'- and 3,4'-DIPB increased with raising reaction temperature: this is due to the isomerization of 4,4'-DIPB.

4. CONCLUSIONS

VPT method was successfully and conveniently applied to synthesize MgAPO-36 with ATS structure. XRD and SEM analyses showed that MgAPO-36 obtained by DGC method has highly pure crystalline phase. Heating protocol, especially intermediate aging time at 105°C played a crucial role for phase formation of pure ATS. NH₃ desorption peaks at high temperature as 250-450°C indicate that magnesium is incorporated into the framework. MgAPO-36 has the Brønsted acidic character by the magnesium in framework. The selectivity for 4,4'-DIPB was about 30-40% among DIPB isomers: this value is quite lower than with MOR. Because the selectivity is higher than the composition in equilibrium, and the isopropylation of BP is controlled by the pores of MgAPO-36. The differences of the

selectivity are not due to their pore entrance but to differences in their pore structure. The cavity in ATS channel can not sufficiently control the transition state to form 4,4'-DIPB.

REFERENCES

1. E. M. Flanigen, B. H. Lok, R. L. Patton, and S. T. Wilson, Pure Appl. Chem. **58**, 1351 (1986).
2. Ch. Baerlocher, W. M. Meier, and D. H. Olson, "Atlas of Zeolite Framework Types", 5th ed., Elsevier, 2001; homepage: http://www.iza-structure.org/databases/
3. J. Smith, J. J. Pluth, and J. K. Andries, Zeolites,**13**, 166 (1993).
4. M. G. Wu, M. W. Deem, S. A. Elomari, R. C. Medrud, S. I. Zones, T. Maesen, C. Kibby, C. -Y. Chen, and I. Y. Chan, J. Phys. Chem. B, **106**, 264 (2002).
5. D. B. Akolekar, J. Catal., **143**, 227 (1993).
6. M. H. Kim, H. X. Li, and M. E. Davis, Micropor. Mater. **1**, 191 (1993).
7. P. R. H. P. Rao and M. Matsukata, Chem. Commun., 1441 (1996).
8. M. Matsukata, M. Ogura, T. Osaki, P. R. H. P. Rao, M. Nomura, and E. Kikuchi., Topics Catal., **9**, 77 (1999).
9. R. Bandyophadhyay, R. K. Ahedi, Y. Kubota, M. Ogawa, Y. Goto, Y. Fukushima, and Y. Sugi, J. Mater. Chem., **11**, 1869 (2001).
10. R. Bandyopadhyay, Y. Kubota, N. Sugimoto, Y. Fukushima, and Y. Sugi, Micropor. Mesopor. Mater., **32**, 81 (1999).
11. T. Tatsumi and N. Jappar, J. Phys. Chem. B, **102**, 7126 (1998).
12. A. Bhaumik and T. Tatsumi, Micropor. Mesopor. Mater., **34**, 1 (2000).
13. T. Takewaki, S. Hwang, H. Yamashita, and M.E. Davis, Micropor. Mesopor. Mater., **32**, 265 (1999).
14. M. V. Giotto, M. da S. Machado, S. P. O. Rios, J. Pérez-Pariente, D. Cardoso, Proc. 12th Intern. Zeolite Conf., IV, 2481 (1998).
15. Y. Sugi, Y. Kubota, T. Hanaoka, and T. Matsuzaki, Catal. Survey Jpn., **5**, 43 (2001).
16. J. -H. Kim, T. Matsuzaki, T. Hanaoka, Y. Kubota, Y. Sugi, M. Matsumoto, and X. Tu, Micropor. Mater., **5**, 113 (1995).
17. Y. Sugi, S. Tawada, T. Sugimura, Y. Kubota, T. Hanaoka, T. Matsuzaki, K. Nakajima, and K. Kunimori, Appl. Catal., **189**, 251 (1999).
18. M. Bandyopadhyay, R. Bandyopadhyay, S. Tawada, Y. Kubota, and Y. Sugi, Appl. Catal. A: General, **225**, 51 (2002).
19. R. K. Ahedi, S. Tawada, Y. Kubota, Y. Sugi, and J. -H. Kim, J. Mol. Catal., **197**, 133 (2003).
20. Y. Sugi, Y. Kubota, A. Ito, H. Maekawa, R. K. Ahedi, S. Watanabe, C. Asaoka, H. -S. Lee, J. -H. Kim, and G. Seo, Catal. Catal., **45**, 114 (2003).
21. unpublished results.